3 Cell Signalling in Urothelium

Peter Woodroffe, Nottingham; Jim Keener, Utah; Oliver Jensen, Nottingham; Andrew Hazel, Alan Jones, Manchester

3.1 Introduction

The urothelium is the highly specialised layer of epithelial cells lining the bladder. It has to maintain a tight barrier against urea and other toxins while accommodating large changes in bladder volume. Consequently, when it is damaged, it has to be able to repair itself rapidly (although under normal conditions there is very low cell turnover rate.) This is controlled by a balance between cell proliferation and differentiation signalling pathways. The study group was asked to model some of the chemical reactions which make up these pathways.

3.1.1 Experimental facts

The experimental results observed by Professor J. Southgate and her group were as follows. See figure 12 for their results.

- Cultured urothelial cells *in vitro* naturally exhibit proliferation.
- The cells only exhibit differentiation when a drug called Troglidazone (TZ) (which mimics the effects of prostaglandins in urine) is administered in the presence of endothelial growth factor (EGF) blocker.
- The differentiation is observed (through expression of membrane proteins called uroplakins) after a wait of 4 days for the gene transcription process to take place.
- The TZ and EGF blocker are administered to the cultured cells for a period of time before being washed off. Less than one hour produces almost no differentiation. Two hours produces a much greater differentiation response. The response then increases slowly with application time, until a maximum is reached. More than 24 hours of TZ appears to give a reduced response.

The study group was asked to explain the initial two hour delay.

3.2 The reaction pathway

The steroid TZ is a ligand for the nuclear hormone receptor PPARγ (peroxisome proliferator activating receptor γ). TZ must cross the cell membrane and the cytoplasm and reach the nucleus, where it binds to and activates PPARγ. Activated PPAR forms a heterodimer with RXR (retinoic acid receptor), and this heterodimer can then bind to PPRE (peroxisome proliferator response element) promoter regions on nuclear DNA. Genes with PPRE promoter regions are thus 'turned on', enabling the production of their respective mRNA's. These mRNA's continue the transcription process, ending up with differentiation (specifically, expression of uroplakins). Phosphorylation of the PPAR-RXR complex (an event that is downstream of EGF administration) deactivates the complex, however, inhibiting differentiation. [2, 7, 4]. See figure 13 for a diagram of this process.

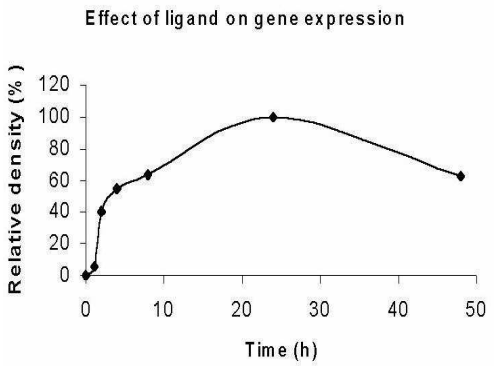

Figure 12: Length of time Troglidazone applied before removal. Vertical axis indicates percentage of maximum differentiation

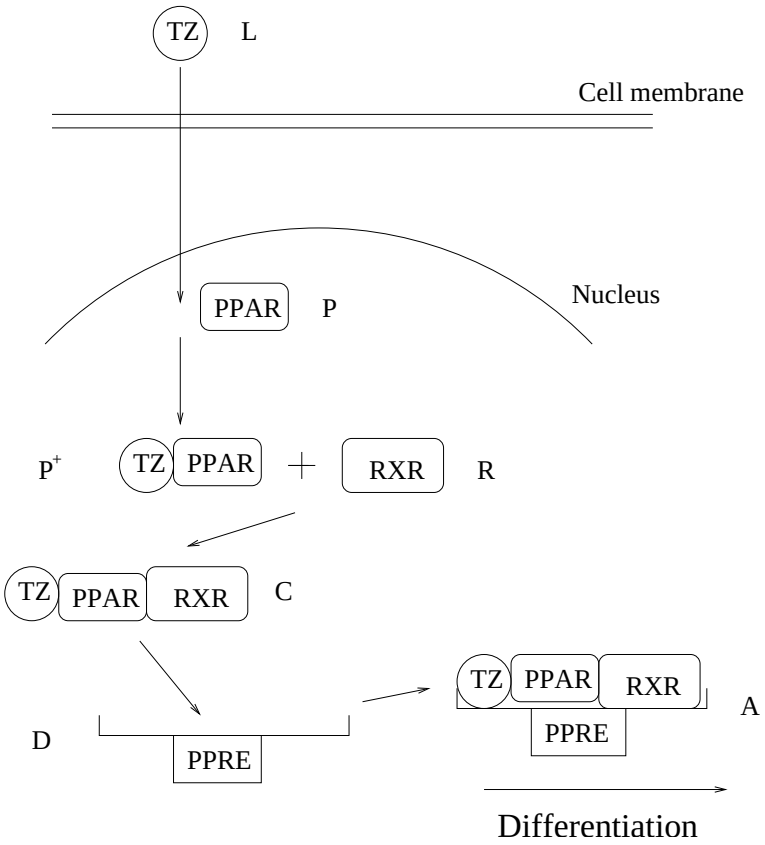

Figure 13: Reaction pathway for PPAR activated differentiation

3.2.1 Variables

The following variables are defined to describe the model:

L : Troglidazone ligand concentration - assumed constant
P : PPAR receptor (inactive) concentration
P^+ : PPAR receptor (active) concentration
R : RXR receptor concentration
C : activated PPAR-RXR complex concentration
C^* : phosphorylated PPAR-RXR complex (inactive) concentration

D : probability that PPRE promoter region on gene is free
A : probability that PPRE is bound to C, $A = 1 - D$
E : EGF concentration.

The reactions are as follows:

$$L + P \underset{k_{-1}}{\overset{k_1}{\rightleftharpoons}} P^+,$$
$$P^+ + R \underset{k_{-2}}{\overset{k_2}{\rightleftharpoons}} C.$$

We also account for a PPAR-RXR complex binding with the free promoter region

$$D \underset{k_-}{\overset{k_+ C}{\rightleftharpoons}} A.$$

In addition we assume that epithelial growth factor leads directly to phosphorylation of the complex via a sequence of pathways, which we lump into the single reaction

$$E + C \underset{k_{-e}}{\overset{k_e}{\rightleftharpoons}} C^*.$$

3.2.2 Mathematical model 1

The reactions can be modelled using the law of mass action with differential equations as follows:

$$\frac{dP^+}{dt} = k_1 LP - k_{-1}P^+ - k_2 P^+ R + k_{-2}C, \tag{3.1}$$
$$\frac{dC}{dt} = k_2 P^+ R - k_{-2}C - k_e EC + k_{-e}C^*, \tag{3.2}$$
$$\frac{dC^*}{dt} = k_e EC - k_{-e}C^*, \tag{3.3}$$

along with conservation laws

$$P + P^+ + C + C^* = P_0, \qquad C + C^* + R = R_0. \tag{3.4}$$

Finally, we view A as the probability that the PPRE site is bound with complex. Thus,

$$\frac{dA}{dt} = k_+ C(1 - A) - k_- A. \tag{3.5}$$

3.2.3 Simplification 1

The value of A will be considered our 'output' variable. The reactions in binding PPAR and RXR and PPAR ligand are likely to be very fast compared with the transcription process. Therefore, the differential equations for P^+ and C can be assumed to be quasi-steady. Assuming that EGF is blocked and so $E = C^* = 0$, this gives

$$\frac{dA}{dt} = k_+ C(1 - A) - k_- A, \tag{3.6}$$
$$0 = k_1 L(P_0 - C - P^+) - k_{-1}P^+, \tag{3.7}$$
$$0 = k_2 P^+(R_0 - C) - k_{-2}C. \tag{3.8}$$

3.2.4 Results 1

Equations (3.7) and (3.8) can be solved to give unique steady state values for C and P^+ which gives the equation for A in the form:

$$\frac{dA}{dt} = a - bA, \tag{3.9}$$

where a and b are positive constants. Solving this with the initial condition $A(0) = 0$, we find

$$A = \frac{a}{b}(1 - e^{-bt}), \tag{3.10}$$

and the graph of this is shown in figure 14.

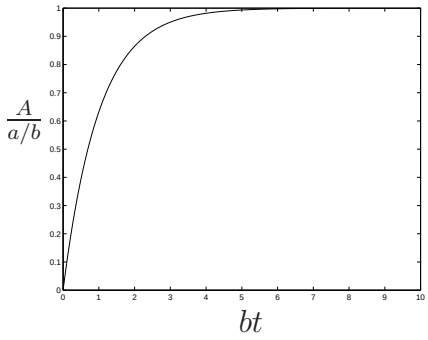

Figure 14: Graph to show result from Model 1

As can be seen from the graph, an initial linear response is observed. This does not agree with the experimental observation that administering TZ and EGF blocker for one hour produces differentiation, but for two hours there is a strong response. So, a literature search was conducted to attempt to find evidence of a feedback system that could give us this delay.

3.3 Feedback mechanism

In adipocytes, fat cells similar to urothelial cells, the PPRE sites activate a particular mRNA which produces fatty acid transport protein (FATP) [5]. This could actively transport the ligand from outside the urothelial cell, all the way in to the nucleus [1, 3]. This creates a positive feeback loop [6]. A second model was constructed, incorporating this loop. See figure 15.

3.3.1 Variables 2

L_e : Extracellular Troglidazone ligand concentration - assumed constant
L : Internal ligand concentration
P : PPAR receptor (inactive) concentration
P^+ : PPAR receptor (active) concentration
R : RXR receptor concentration
C : activated PPAR-RXR complex concentration
C^* : phosphorylated PPAR-RXR complex (inactive) concentration
A : probability that PPRE is bound to C
E : EGF concentration

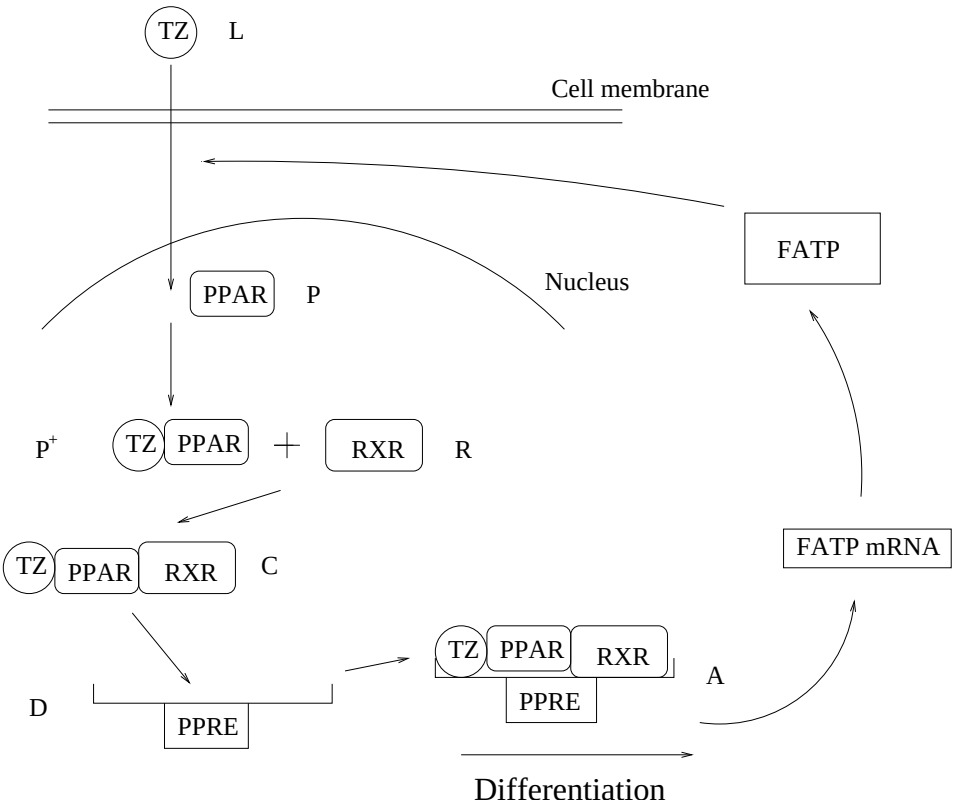

Figure 15: Reaction pathway for FATP mediated PPAR activated differentiation

F : FATP concentration
F_m : FATP mRNA concentration.

The reactions are now as follows:

$$\begin{aligned}
L_e &\xrightarrow{F} L, \\
L + P &\underset{k_{-1}}{\overset{k_1}{\rightleftharpoons}} P^+, \\
P^+ + R &\underset{k_{-2}}{\overset{k_2}{\rightleftharpoons}} C, \\
&\xrightarrow{A} F_m, \\
&\xrightarrow{F_m} F, \\
E + C &\underset{k_{-e}}{\overset{k_e}{\rightleftharpoons}} C^*.
\end{aligned}$$

3.3.2 Mathematical model 2

The system of differential equations therefore becomes

$$\frac{dL}{dt} = \frac{V_L L_e F}{K_F + L_e} - k_1 LP, \tag{3.11}$$
$$\frac{dP}{dt} = k_{-1}P^+ - k_1 LP, \tag{3.12}$$
$$\frac{dP^+}{dt} = k_1 LP - k_{-1}P^+ - k_2 P^+ R + k_{-2}C, \tag{3.13}$$
$$\frac{dF_m}{dt} = k_3 A - k_{-3}F_m + \epsilon, \tag{3.14}$$
$$\frac{dF}{dt} = k_4 F_m - k_{-4}F, \tag{3.15}$$
$$\frac{dC^*}{dt} = k_e EC - k_{-e}C^*, \tag{3.16}$$
$$\frac{dA}{dt} = k_+ C(1-A) - k_- A, \tag{3.17}$$

along with conservation laws

$$P + P^+ + C + C^* = P_0, \qquad C + C^* + R = R_0. \tag{3.18}$$

The ODEs were once again obtained using the law of mass action, except for the movement of PPAR ligand into the cell. This rate would increase with the concentration of ligand, but is likely to level off, at high values of L_e, which is why the first term in equation (3.11) was used. V_L represents the rate of uptake into the cell, K_F is the equilibrium constant for the uptake of TZ by FATP. The small parameter ϵ was added to equation (3.14) to model a small source term for the production of FATP mRNA.

3.3.3 Simplification 2

The value of F will now be considered our 'output' variable, since it is the product of a mRNA, as would be the next stage in the differentiation pathway. The slowest processes here are likely to be the production of F from its messenger RNA, and the degradation of C^*. Thus, we take all other equations to be steady state, giving the two ODEs (3.15,3.16) subject to

$$0 = V_L \frac{F L_e}{K_F + L_e} - k_1 LP, \tag{3.19}$$
$$0 = k_1 LP - k_{-1}P^+ - k_2 P^+ R + k_{-2}C, \tag{3.20}$$
$$0 = k_{-1}P^+ - k_1 LP, \tag{3.21}$$
$$0 = k_3 A - k_{-3}F_m + \epsilon, \tag{3.22}$$
$$P_0 = P + P^+ + C + C^*, \tag{3.23}$$
$$R_0 = C + C^* + R, \tag{3.24}$$
$$0 = k_+ C(1-A) - k_- A. \tag{3.25}$$

After simplification, we get

$$\frac{dF}{dt} = \frac{k_4}{k_{-3}} \left(\frac{k_3 (R_0 - C^*) L_f F}{L_f F (R_0 - C^*) + K L_f F + K K_{12}} + \epsilon \right) - k_{-4} F, \tag{3.26}$$
$$\frac{dC^*}{dt} = \frac{k_e L_f F (R_0 - C^*) E}{(K_{12} + L_f F)} - k_{-e} C^*, \tag{3.27}$$

where

$$K = \frac{k_-}{k_+}, \qquad K_{12} = \frac{k_- k_{-2}}{k_2}, \qquad L_f = \frac{V_L L_e}{K_F + L_e}.$$

3.3.4 Parameter values

Two parameters were obtained from the literature [5]

$$K_F = 0.2\ \mu\text{M}, \qquad V_L = 0.6\ \text{fmol/cell/min}.$$

The other parameters were estimated as follows

$$\frac{k_4}{k_{-3}} = 30, \qquad k_3 = 0.5\ \text{Ms}^{-1}, \qquad L_f = 0.5\ \text{s}^{-1}, \qquad R_0 = 1,$$

$$K = 10\ \text{M}, \qquad K_{12} = 1\ \text{Ms}^{-1}, \qquad \epsilon = 10^{-5}\ \text{Ms}^{-1}, \qquad k_{-4} = 1\ \text{s}^{-1},$$
$$k_e = 20\ \text{M}^{-1}\text{s}^{-1}, \qquad k_{-e} = 0.5\ \text{s}^{-1}.$$

3.3.5 Numerical results 2

Case 1 - $E = 0$

This model (3.26,3.27) was simulated in MatLab. The phase portrait for $E = 0$ can be seen in figure 16.

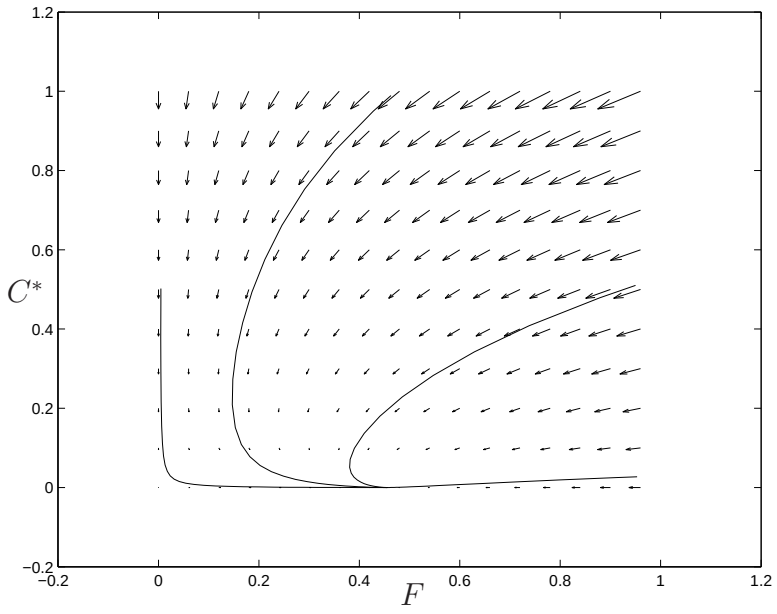

Figure 16: Phase plane portrait for $E = 0$

Figure 16 displays the steady state at $F \approx 0.45, \quad C^* = 0$. This shows that when EGF is blocked, there is an output of F. To see a close up view of the fixed point, see figure 17.

Case 2 - $E = 10$

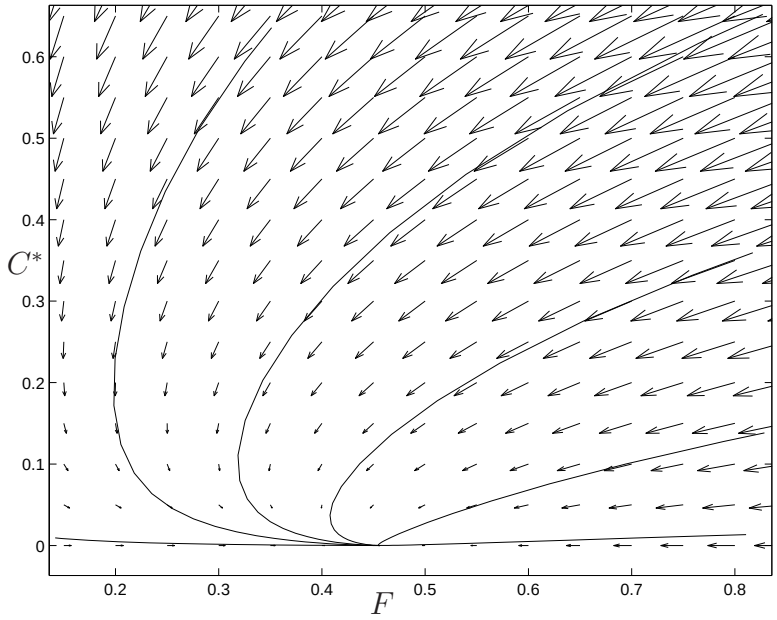

Figure 17: Detailed view of the fixed point for $E = 0$

Now, to check that the model suppresses differentiation when EGF is applied, let $E = 10$. Figure 18 displays the steady state at $F \approx 0, \quad C^* \approx 0.44$. Hence, when EGF is applied, the output of F decreases to zero. And so differentiation will not occur. Once again, a more detailed picture of the steady state can be seen in figure 19.

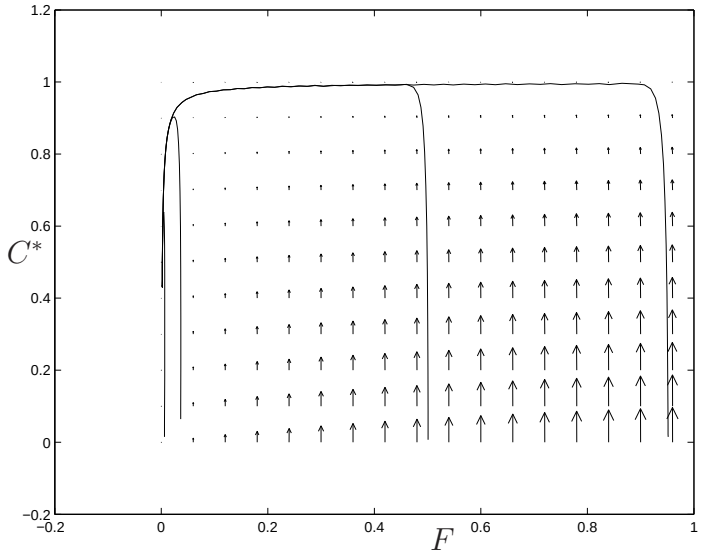

Figure 18: Phase plane portrait for $E = 10$

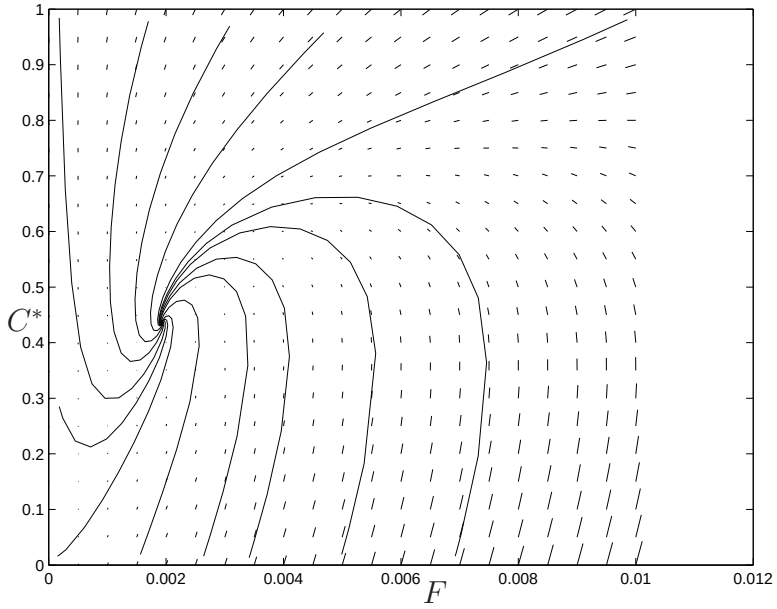

Figure 19: Detailed view of the fixed point for $E = 10$

3.3.6 Time course results

To illustrate the model, the parameter values from 1.3.4 were taken. Figures 20-22 show corresponding results, from three simulated experiments.

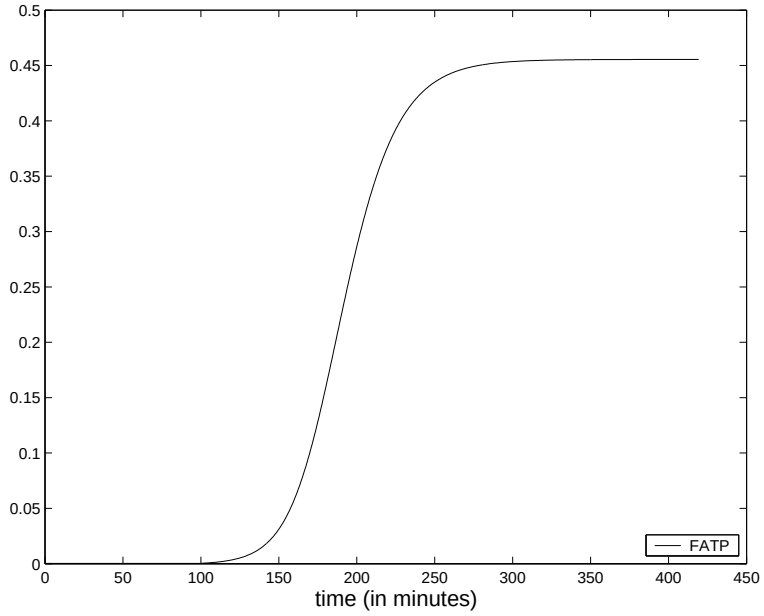

Figure 20: $E = 0, \quad L_e = H(t - 100)$, where $H(t)$ is the Heaviside function

- Figure 20. We suppose TZ is applied at time 100, with the EGF blocked ($E = 0$). There is a small response after an hour ($F \approx 0.05$ at $t = 160$) and an almost maximal response after two hours ($F \approx 0.45$ at $t = 220$).

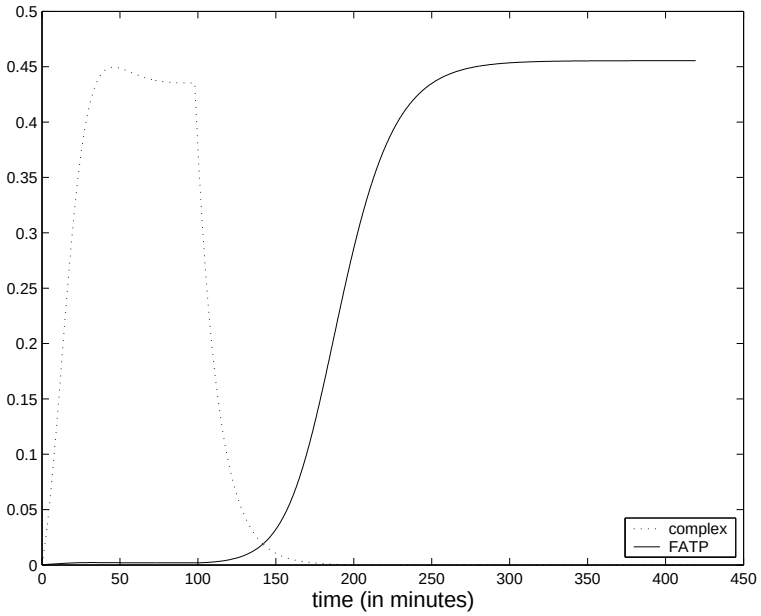

Figure 21: $E = 10H(t-100), \quad L_e = 1.$

- Figure 21. Initially, both EGF and drug are present, and there is no FATP response. At $t = 100$ the EGF is blocked ($E = 0$) and the response is the same as for the first case of $E = 0$ at all time.

- Figure (22). In this experiment, the EGF was left on all the time, and the drug was applied at $t = 100$ to demonstrate that there was no response in this case either.

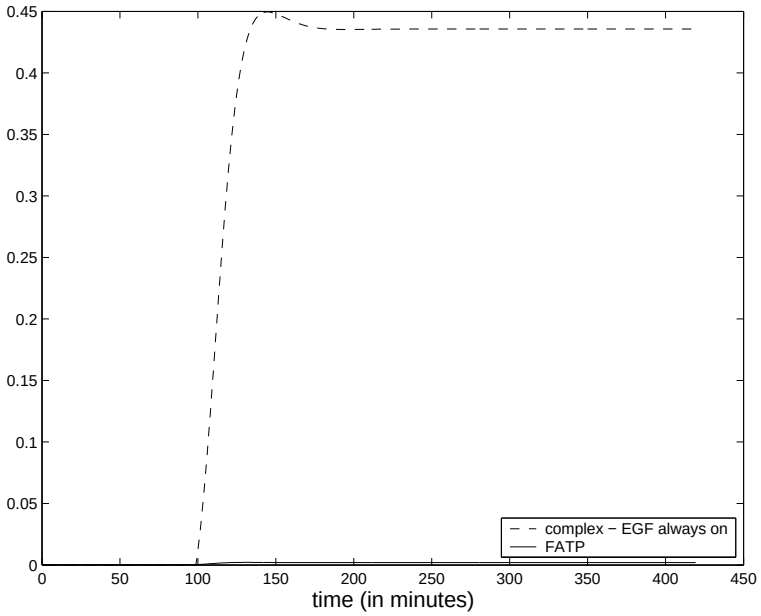

Figure 22: $E = 10, \quad L_e = H(t-100).$

3.4 Conclusion

As can be seen from the results, the model matches the experimental observations of a very small response after one hour of drug application and a much greater response after two hours of drug application. We have shown that the first model of a simple drug activation pathway was not sufficient to achieve this effect and that the presence of a feedback loop is required. We have argued the case and demonstrated the possibility of FATP causing such a loop. It remains to be seen whether this loop or perhaps another actually operates in urothelium.

Many of the parameters used in the model had to be estimated from knowledge of rates of similar reactions, often in non-urothelial cells. Hence, the model is more qualitative than quantitative, and hopefully more laboratory work can be done to gain accurate parameter and rate values to allow us to model the system thoroughly.

Acknowledgements

The urothelium group would like to thank the following people for their contributions during the week, especially the biologists: Jenny Southgate and Clare Varley. On the mathematical side we thank: Colin Bolton, Jan Bouwe van den Berg, April Chen, Nick Hill, John King, Aisling Metcalfe, and anyone else we've forgotten.

References

[1] Desvergne, B. and Wahli, W. (1999) Peroxisome Proliferator-Activated Receptors: Nuclear Control of Metabolism. *Endo. Rev* **20** 649–688

[2] Houseknecht, K.L., Cole, B.M. and Steele, P.J. (2002) Peroxisome Proliferator-Activated Receptor-γ and its Ligands: A Review. *Dom. An. Endocrin.* **22** 1–23

[3] Martin, G., Poirier, H., Hennuyer, N., Crombie, D., Fruchart, J-C., Heyman, R.A., Besnard, P. and Auwerx, J. (2000) Induction of the Fatty Acid Transport Protein 1 and Acyl-CoA Synthase Genes by Dimer-selective Rexinoids Suggests That the Peroxisome Proliferator-activated Receptor-Retinoid X Receptor Heterodimer Is Their Molecular Target. *J. Biol. Chem* **275** 12612–12618

[4] Mueller, E., Sarraf, P., Tontonoz, P., Evans, R.M., Martin, K.J., Zhang, M., Letcher, C., Singer, S. and Speigelman, B.M. (1998) Terminal Differentiation of Human Breast Cancer through PPARγ. *Mol. Cell* **1**, 465–470

[5] Shaffer, J.E. and Lodish, H.F. (1994) Expression Cloning and Characterization of a Novel Adipocyte Long Chain Fatty Acid Transport Protein. *Cell* **79** 427–436

[6] Stahl, S., Gimeno, R.E., Tartaglia, L.A. and Lodish, H.F. (2001) Fatty acid transport proteins: a current view of a growing family. *TRENDS in Endo. and Meto.* **12** 266–273

[7] Wang, A.C.C., Dai, X., Luu, B. and Conrad, D.J. (2001) Peroxisome Proliferator-Activated Receptor-γ Regulates Airway Epitelial Cell Activation. *Am. J. Respir. Cell Mol. Biol.* **24**, 688–693.